Available online at www.sciencedirect.com
SCIENCE DIRECT®
ELSEVIER
International Journal of Solids and Structures 43 (2006) 4452–4464
INTERNATIONAL JOURNAL OF SOLIDS and STRUCTURES
www.elsevier.com/locate/ijsolstr

Toughening under non-uniform ferro-elastic domain switching

Yuanqing Cui, Wei Yang *

Department of Engineering Mechanics, Tsinghua University, Beijing 100084, China

Received 8 March 2005; received in revised form 18 May 2005
Available online 11 July 2005

Abstract

The existing models of switch-toughening seldom consider the effect of non-uniform ferro-elastic domain switching in the vicinity of a crack. To explore this issue, an evolution law for the volume fraction of the switched portion under applied electromechanical loading is established from the minimum energy principle. Based on this law, a switching model capable of dealing with the non-uniform distribution of switching strain is developed. The domain switching zone is divided into a saturated inner core and an active surrounding annulus. Mono-domain solution of ferro-elastic toughening is obtained under the model of small scale domain switching. Toughening for ferroelectrics with different poling states is estimated via Reuss type approximation. Two sets of solutions are obtained according to spherical and cylindrical inclusions. The interval of toughening defined by these two models covers the range of experimental data. The same conclusion is reached for the size of the switching zone.

Keywords: Piezoelectric; Ceramics; Crack; Stress intensity factor; Toughness

1. Introduction

While recent decades have seen progressive applications of ferroelectric materials in wide aspects, such as sensors, actuators and smart structures, the intrinsic brittleness of ferroelectric materials leads to grave concerns with respect to reliability issues. Among them, ferro-elastic/ferroelectric toughening is a major remedy. The assumption of uniform domain switching is typically made within a switching zone in the toughening calculation. This assumption traces its source back to what was made in the pioneering work of transformation toughening for zirconia-containing ceramics. In transformation toughening, it is often assumed that the transformation strain remains constant within the transformed zone and vanishes outside

* Corresponding author. Tel.: +86 10 6278 2642; fax: +86 10 6278 1824.
E-mail address: yw-dem@tsinghua.edu.cn (W. Yang).

0020-7683/$ - see front matter
doi:10.1016/j.ijsolstr.2005.05.015

it. Thus a strong step-like discontinuity exists in the magnitude of strain across the transformation boundary. This step-like jump is probably unrealistic, and a gradual change in the volume fraction of the transformed material across the process zone is to be expected (Hannink et al., 2000).

Budiansky et al. (1983) first distinguished the fully and the partially transformed zone. They introduced two types of transformation constitutive relations: super-critical and sub-critical. Experimental evidences reveal a fact that the realistic volume fraction is not uniform within a transformation zone (Cox et al., 1988; Marshall et al., 1990), and the volume fraction within the zone decreases continuously with increasing distance from the crack tip. Evaluation of the shielding were made for actual transformation zone profile based on size distribution of the transforming particles (Hsueh and Becher, 1988), as well as on the experimental measurements of the zone size (Yu et al., 1992). In contrast to the richness of literatures about calculation towards super-critical type transformation, available toughening results for sub-critical one are few and far between. This is also the case for ferro-elastic toughening.

The concept of non-uniform domain switching was elucidated qualitatively by Kolleck et al. (2000) for ferroelectric domain switching induced by electric field parallel to the crack front. The non-uniformity in ferro-elastic domain switching was experimentally confirmed by Förderreuther et al. (2002) and Hackemann and Pfeiffer (2003). The existence of a transition area of polarization switching was verified by many experiments (e.g. Cao and Evans, 1993; Schäufele and Härdtl, 1996) for ferroelectrics. The idea of dividing the ferro-elastically switched region into a saturated inner core and a transitional outer layer was proposed by Reece and Guiu (2002). However, no analytical effort has been devoted to exploring the toughening effect of non-uniform domain switching.

The present work deals with the fully and partially switchings by introducing a saturated switching core that encloses the crack tip and is surrounded by a partially switched annulus. Different criteria are proposed for the saturated and the transitional switching boundaries in Section 2. Two sets of solutions are obtained for spherical and cylindrical inclusions anticipated in the evolution of non-uniform volume fraction. Two-dimensional weight function is introduced to calculate the toughening induced by non-uniform ferro-elastic domain switching in Section 3. In Section 4, toughening of mono-domain is calculated under the framework of small scale domain switching. The toughening calculation is conducted for the asymptote of R-curve for the steady-state crack growth. The mono-domain solution is used to construct toughening for ferroelectric ceramics via Reuss type approximation and an orientation distribution function. Evaluation is performed for ferroelectrics with un-poled and two poled configurations. Two sets of solutions are obtained corresponding to spherical and cylindrical inclusions. The steady state toughness and the size of the switching zone measured in experiment fall within the interval defined by two sets of solutions.

2. Evolution law of volume fraction for non-uniform ferro-elastic domain switching

Attention here is restricted to in-plane deformation and loading. Cartesian coordinates are introduced, such that x_1 is along the crack direction and x_2 is normal to it. We start from the simple case of mono-domain ferroelectrics. If the mono-domain forms an angle ϕ with respect to x_1, after the complete 90° domain switching, the corresponding switching strain is (Yang and Zhu, 1998)

$$\Delta\varepsilon_{ij} = \varepsilon_{\mathrm{sp}}\tilde{\varepsilon}_{ij} = \varepsilon_{\mathrm{sp}}\begin{bmatrix} -\cos 2\phi & -\sin 2\phi \\ -\sin 2\phi & \cos 2\phi \end{bmatrix}, \quad \varepsilon_{\mathrm{sp}} \approx \frac{c-a}{a}, \tag{1}$$

where $\varepsilon_{\mathrm{sp}}$ denotes the spontaneous polarization strain, $\tilde{\varepsilon}_{ij}$ the orientation dependent angular distribution, and c, a the lattice parameters of tetragonal ferroelectric phase. Mono-domain is easily obtained in single crystal samples and the domain could switch entirely with the action of applied field above the coercive field. But the case is different for grains in ferroelectric ceramics. Two questions have to be answered: when the switching is activated and how many of the domains will switch under the applied load. Yang et al.

(2001b) and Yang (2002) derived an expression for the system energy change, as described in detail in (A.1) of Appendix A, for a switched spherical grain with banded structure embedded in an otherwise infinite ferroelectric medium subjected to applied electromechanical loading.

Generalizing (A.1) into arbitrary in-plane loading, one may convert the mechanical work for domain switching, elucidated in Eq. (1), as

$$\sigma_{ij}\Delta\varepsilon_{ij} = 2\varepsilon_{\mathrm{sp}}\sigma_{\mathrm{DS}}, \quad \sigma_{\mathrm{DS}} = \frac{\sigma_{22}-\sigma_{11}}{2}\cos 2\phi - \sigma_{12}\sin 2\phi. \tag{2}$$

The quantity, σ_{DS}, not only measures the external work during 90° domain switching but also acts as a stress combination to control the degree of domain switching. As schematically depicted in Fig. 1, the stress combination σ_{DS} corresponds to the shear stress component in a new coordinate system $x_1'x_2'$ rotating anti-clockwise by an angle of $\pi/4+\phi$. In Fig. 1, P_0 refers to the polarization vector with initial orientation ϕ and P_{90} the polarization vector after 90° domain switching. It is noteworthy that only the anti-clockwise 90° domain switching is shown in Fig. 1. For the clockwise case, the same switching strain tensor like Eq. (1) holds, thus rendering the distinction of two cases unnecessary in the subsequent calculations of ferro-elastic domain switching. The subscript "DS" stands for domain switching. Since σ_{DS} controls the domain switching, other stress elements in Fig. 1 are omitted for clarity.

As the first step, by neglecting the insignificant second item in (A.1) and combining the threshold quantity in domain switching, one obtains following explicit expression

$$V_{90} = \frac{15(1-\nu^2)}{2(7-5\nu)E}\frac{1}{\varepsilon_{\mathrm{sp}}^2}[\sigma_{ij}\Delta\varepsilon_{ij}(\phi) - W_{\mathrm{th}}] = \frac{15(1-\nu^2)}{(7-5\nu)E}\frac{1}{\varepsilon_{\mathrm{sp}}}[\sigma_{\mathrm{DS}} - \sigma_{\mathrm{th}}] \tag{3}$$

for V_{90}, the volume fraction of the portion that experiences 90° domain switching, for the case of purely mechanical loading. In (3), E is the Young's modulus, ν the Poisson's ratio, and W_{th} the threshold energy. One may further defines a threshold stress as $\sigma_{\mathrm{th}} = W_{\mathrm{th}}/2\varepsilon_{\mathrm{sp}}$, which is equivalent to the concept of threshold energy. Eq. (3) is derived for a fully constrained spherical grain (or inclusion). For a cylindrical grain (or inclusion) unconstrained along x_3 direction, a similar expression is arrived by changing the factor $15(1-\nu^2)/(7-5\nu)$ above to $16(1-\nu^2)/3$. Eq. (3) acts as the governing equation for the evolution of volume fraction under mechanical loading. The switching criterion implied in (3) is

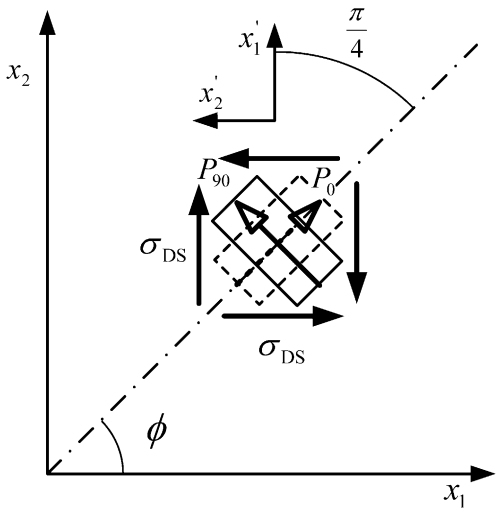

Fig. 1. Switch-controlling characteristic stress σ_{DS} and related domain switching for a special case of $\phi = \pi/4$.

$$\sigma_{DS} \geqslant \sigma_{th}. \tag{4}$$

On the other hand, load-dependent volume fraction is solved through minimizing (A.1) under prescribed load. We illustrate the usage of this criterion by considering a special loading of unidirectional compression. The minimum energy is sought through the optimization method for the applied compressive stress. As a result, one obtains a dotted curve (shown in Fig. 2) between the volume fraction, V_{90}, and the stress combination σ_{DS}, which is a half of the compressive stress in magnitude. For the ease of derivation, an explicit formula like (3) is preferred and it should correlate the exact solution. Combining the linear relation in (3) and the incubation regime of domain switching, one may propose the following piecewise function

$$V_{90} = \begin{cases} 0 & \sigma_{DS} < \sigma_{th}, \\ V_{90}^0 + (1 - V_{90}^0)\frac{\sigma_{DS} - \sigma_{th}}{\sigma_f - \sigma_{th}} & \sigma_{th} \leqslant \sigma_{DS} < \sigma_f, \\ 1 & \sigma_{DS} \geqslant \sigma_f. \end{cases} \tag{5}$$

This approximation is represented by the solid line in Fig. 2 where V_{90}^0 and σ_{th} are also marked. In Eq. (5) and/or Fig. 2, V_{90}^0 is the uniform component of V_{90} and remains constant within the switching zone, $(1 - V_{90}^0)(\sigma_{DS} - \sigma_{th})/(\sigma_f - \sigma_{th})$ is the non-uniform part of V_{90} and governed by the characteristic stress σ_{DS}, and σ_f means the stress level causing complete domain switching, i.e. $V_{90} = 1$. The presence of V_{90}^0, though behaved as a step-like discontinuity along the switching boundary, is rather weak if compared with the jump in the completely uniform switching model.

Eqs. (4) and (5) depict the evolution equation for ferro-elastic domain switching. Beside the correlation with exact solution by Yang et al. (2001b), this piecewise linear relation also meets the experiment data of zirconia transformation by Marshall et al. (1990). The mentioned experiment also supported the existence of a saturated region. The saturation of ferro-elastic switching strain, ε_p^{max}, links to the saturation in ferroelectrics in experiments (Cao and Evans, 1993; Schäufele and Härdtl, 1996), as shown schematically in Fig. 3. It is rather difficult to achieve complete domain switching for grains of ferroelectric ceramics even in a saturation state. Accordingly, we assume that the maximum or saturated value of volume fraction is acquired under the amplitude of $\sigma = \sigma_{max}$ with the corresponding volume fraction being $V_{90}^0 + (1 - V_{90}^0)(\sigma_{max} - \sigma_{th})/(\sigma_f - \sigma_{th})$. The value of σ_{max} is determined by substituting the saturated volume fraction V_{90}^{max} from experiment and σ_{th} into (5).

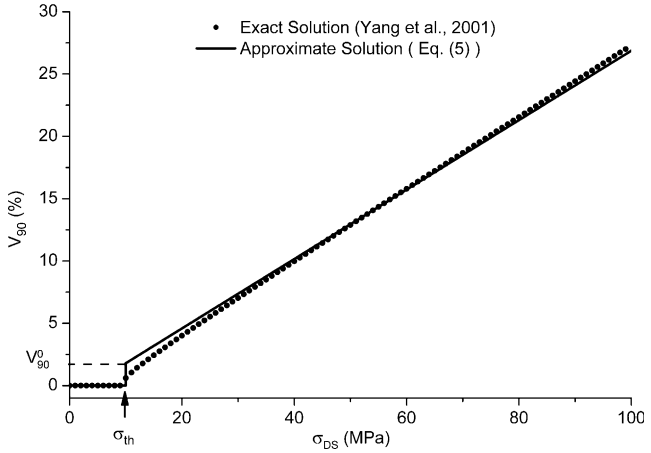

Fig. 2. Comparison of the evolution law of V_{90} versus σ_{DS}. The dotted curve denotes prediction by the exact energy calculation of (A.1) and the solid line represents linearized approximation of Eq. (5).

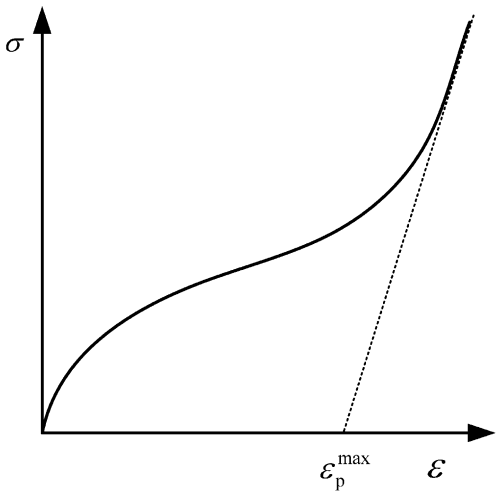

Fig. 3. Schematics of the stress–strain curves as measured from the experiment of compressive ferroelectric specimen.

With the introduction of σ_{max}, Eq. (5) implies the saturation phenomenon in the vicinity of a crack tip, surrounded by a non-uniform partial switching zone, as caused by the stress singularity near a crack tip. A dividing boundary between these two regions is termed the saturated switching boundary and determined by σ_{max}. Within the saturated region, the volume fraction exhibits the maximum value and remains constant. The dividing boundary between the partially switched zone and non-switched zone is termed the switching boundary and determined by σ_{th}. Within the transition region, the volume fraction decreases continuously from V_{90}^{max} along the saturated boundary to V_{90}^{0} along the switching boundary with increasing distance from the crack tip. Incorporating the quantity of volume fraction into the formula of switching strain, one may write the average strain tensor as

$$\Delta\bar{\varepsilon}_{ij} = V_{90}\Delta\varepsilon_{ij}, \tag{6}$$

where the super-imposed bar in $\Delta\bar{\varepsilon}_{ij}$ indicates the average.

3. Toughening from ferro-elastic domain switching

In this work, consideration is restricted to plane strain crack problems of mode I. In linear elastic fracture mechanics, mode I crack-tip stress field reads

$$\sigma_{ij} = \frac{K^{\infty}}{\sqrt{2\pi r}}\tilde{\sigma}_{ij}(\theta) \tag{7}$$

and the angular distribution function $\tilde{\sigma}_{ij}(\theta)$ could be found in any fracture mechanics textbook. For domain switching activated by the crack-tip stress field, one may substitutes Eqs. (1) and (7) into Eq. (2) to get the following expression for the switch-controlling stress

$$\sigma_{DS} = \frac{K^{\infty}}{2\sqrt{2\pi r}}\sin\theta\sin\left(\frac{3}{2}\theta - 2\phi\right). \tag{8}$$

From the switching criterion, the contour lines of volume fraction inside a switching zone are given by

$$\sqrt{r} = \frac{K^{\infty}}{2\sqrt{2\pi}\sigma_{DS}}\sin\theta\sin\left(\frac{3}{2}\theta - 2\phi\right). \tag{9}$$

One gets the switching boundary, R_{trans}, by setting $\sigma_{\text{DS}} = \sigma_{\text{th}}$ and the saturated switching boundary, R_{sat}, by setting $\sigma_{\text{DS}} = \sigma_{\max}$. Details of the geometries of the domain switching zone are furnished in Appendix B. From (B.3), the maximum half-height of the saturated switching boundary, $h^{\max}_{\text{saturated}}$, and that of the switching boundary, $h^{\max}_{\text{switch}}$, are obtained. Since un-perturbed elastic solution (7) is exploited, Eq. (9) gives the first order approximation of the switching boundary. Smooth transition of switching strain from the crack-tip to the switching boundary along a radial line merits the present non-uniform switching model more realistic than a uniform model. We now in a position to consider the contribution of ferro-elastic domain switching to the crack tip toughening. It is well known that the stress intensity factor at a crack tip, K_{tip} is shielded from the remotely applied, K^{∞}, as

$$K_{\text{tip}} = K^{\infty} + \Delta K \tag{10}$$

by a toughness increment, ΔK, exerted by the constraining stress against domain switching. The criterion of stress intensity factor is adopted for crack initiation. The cracking starts when the crack-tip stress intensity factor K_{tip} reaches the intrinsic fracture toughness $K_{\text{intrinsic}}$.

To calculate the ferro-elastic toughening induced by the non-uniform switching area, one needs to exploit two-dimensional weight function. Rice (1985) derived the three-dimensional weight functions of tensile mode for the half-plane crack. Bueckner (1987) obtained a complete set of three-dimensional weight functions for half-plane and penny-shaped cracks. Based on their works, Gao (1989) gave a more concise expression for the interaction between a crack-tip and a source of internal stress. The degenerated mode I weight function for a half-plane crack in an otherwise infinite elastic body was given by Gao (1989) as

$$H_{ij} = \frac{1}{16\sqrt{2\pi}(1-\nu)} \frac{1}{r^{\frac{3}{2}}} \widetilde{H}_{ij}, \tag{11}$$

$$\begin{Bmatrix} \widetilde{H}_{11} \\ \widetilde{H}_{22} \\ \widetilde{H}_{12} \end{Bmatrix} = \begin{Bmatrix} \cos(3\theta/2) + 3\cos(7\theta/2) \\ 7\cos(3\theta/2) - 3\cos(7\theta/2) \\ -3\sin(3\theta/2) + 3\sin(7\theta/2) \end{Bmatrix}. \tag{12}$$

The formula of transformation toughening can be converted to the ferro-elastic case as

$$\Delta K = \frac{E}{1+\nu} \int_A H_{ij} \Delta \bar{\varepsilon}_{ij} \, \mathrm{d}A = \frac{3E\varepsilon_{\text{sp}}}{4\sqrt{2\pi}(1-\nu^2)} \int_A V_{90} \sin\theta \sin\left(\frac{5\theta}{2} - 2\phi\right) \frac{1}{r^{\frac{3}{2}}} \, \mathrm{d}A, \tag{13}$$

where A represents the whole switching area. In (13), as commonly accepted in transformation case (e.g. Budiansky et al., 1983; Lambropoulos, 1986), we assume the modulus of the switched region is roughly the same as that of the un-switched matrix.

Combining Eqs. (5) and (13), one may divide the toughness increment into the contribution from the uniform switching, $\Delta K^{\text{uniform}}$, and the contribution from the non-uniform switching $\Delta K^{\text{non-uniform}}$:

$$\Delta K = \Delta K^{\text{uniform}} + \Delta K^{\text{non-uniform}}. \tag{14}$$

In the calculation of $\Delta K^{\text{non-uniform}}$, one divides the whole switching zone into a saturated core and a transitional annulus. The non-uniform toughness increment consists of contributions from them as

$$\Delta K^{\text{non-uniform}} = \Delta K^{\text{transition}} + \Delta K^{\text{saturated}}. \tag{15}$$

4. Results and discussions

The knowledge presented in the last two sections paves the way for toughening calculations. We start our discussions of the ferro-elastic toughening from the uniform and the non-uniform domain switching of a stationary crack.

4.1. Stationary crack

For the uniform switching, substituting V_{90}^0 into Eq. (13), one obtains the toughness increment

$$\Delta K^{\text{uniform}} = \frac{3E\varepsilon_{\text{sp}}}{4\sqrt{2\pi}(1-\nu^2)}\int_{\theta_1}^{\theta_2}\int_0^{R_{\text{trans}}} V_{90}^0 \sin\theta \sin\left(\frac{5\theta}{2}-2\phi\right)\frac{1}{\sqrt{r}}\,\mathrm{d}r\,\mathrm{d}\theta$$
$$= \frac{EV_{90}^0\varepsilon_{\text{sp}}K_{\text{app}}}{32\pi(1-\nu^2)\sigma_{\text{th}}}[\Theta(\theta_2)-\Theta(\theta_1)], \tag{16}$$

where

$$\Theta(\theta) = \frac{1}{4}[6\sin\theta + 3\sin(2\theta-4\phi) - 2\sin 3\theta - 3\sin(4\theta-4\phi) + \sin(6\theta-4\phi)]. \tag{17}$$

Similarly, the contribution from the saturated region of non-uniform switching is

$$\Delta K^{\text{saturated}} = \frac{45(1-V_{90}^0)}{4\sqrt{2\pi}(7-5\nu)}\int_{\theta_1}^{\theta_2}\int_0^{R_{\text{sat}}} (\sigma_{\max}-\sigma_{\text{th}})\sin\theta\sin\left(\frac{5\theta}{2}-2\phi\right)\frac{1}{\sqrt{r}}\,\mathrm{d}r\,\mathrm{d}\theta$$
$$= \frac{15(1-V_{90}^0)K^{\infty}}{32\pi(7-5\nu)}\left(1-\frac{\sigma_{\text{th}}}{\sigma_{\max}}\right)[\Theta(\theta_2)-\Theta(\theta_1)], \tag{18}$$

and the contribution from the transitional region of non-uniform switching is

$$\Delta K^{\text{transition}} = \frac{45(1-V_{90}^0)}{4\sqrt{2\pi}(7-5\nu)}\int_{\theta_1}^{\theta_2}\int_{R_{\text{sat}}}^{R_{\text{trans}}} (\sigma_{\text{DS}}-\sigma_{\text{th}})\sin\theta\sin\left(\frac{5\theta}{2}-2\phi\right)\frac{1}{\sqrt{r}}\,\mathrm{d}r\,\mathrm{d}\theta$$
$$= \frac{15(1-V_{90}^0)K^{\infty}}{32\pi(7-5\nu)}\left(\ln\frac{\sigma_{\max}}{\sigma_{\text{th}}}-1+\frac{\sigma_{\text{th}}}{\sigma_{\max}}\right)[\Theta(\theta_2)-\Theta(\theta_1)]. \tag{19}$$

Combination of Eqs. (15), (18) and (19) leads to

$$\Delta K^{\text{non-uniform}} = \frac{15(1-V_{90}^0)K^{\infty}}{32\pi(7-5\nu)}\ln\frac{\sigma_{\max}}{\sigma_{\text{th}}}[\Theta(\theta_2)-\Theta(\theta_1)] \tag{20}$$

for the toughness contribution from non-uniform switching.

Substitutions of Eqs. (16) and (20) into Eq. (14) gives rise to

$$\Delta K = \eta[\Theta(\theta_2)-\Theta(\theta_1)]K^{\infty} \tag{21}$$

for the toughening from the combinations of uniform and non-uniform switching, where a non-dimensional constant η reads

$$\eta = \frac{1}{32\pi}\left[\frac{EV_{90}^0\varepsilon_{\text{sp}}}{(1-\nu^2)\sigma_{\text{th}}} + \frac{15(1-V_{90}^0)}{7-5\nu}\ln\frac{\sigma_{\max}}{\sigma_{\text{th}}}\right]. \tag{22}$$

The toughness solution (21) for non-uniform switching reduces to the solution for uniform switching by Yang and Zhu (1998) if one sets $\sigma_{\text{th}} = \sigma_{\max}$ and $V_{90}^0 = V_{90}^{\max}$ in (22).

For the toughening of the whole switching zone, one arrives at the following expression for a stationary crack,

$$\Delta K = \eta[\Theta(\theta_{\text{f}}^+)-\Theta(\theta_{\text{i}}^+)+\Theta(\theta_{\text{f}}^-)-\Theta(\theta_{\text{i}}^-)]K^{\infty}. \tag{23}$$

The definitions and expressions for the initial and the final angles $\theta_{\text{i}}^{\pm}$ and $\theta_{\text{f}}^{\pm}$ can be found in Appendix B. Substitution of $\theta_{\text{i}}^{\pm}$ and $\theta_{\text{f}}^{\pm}$ in (B.1) and (B.2) into (23) yields

$$\Delta K = 0. \tag{24}$$

Namely the constraining stress from domain switching bears no effect on the apparent fracture toughness for a stationary crack.

4.2. Growing crack

Next consider the switch-induced toughening for a growing crack. The switching zone is divided into a frontal zone and a wake such that

$$\Delta K = \Delta K_{\text{front}} + \Delta K_{\text{wake}}. \tag{25}$$

Both zones comprise the transitional and the saturated switching regions.

The frontal zone resembles the structure delineated for a stationary crack. Substituting the corresponding angles in (B.1), (B.2) and (B.4) for the upper and the lower halves of the switched zone into (23), one has

$$\Delta K_{\text{front}} = \eta[\Theta(\theta^+_{\max}) - \Theta(\theta^+_{\text{i}}) + \Theta(\theta^-_{\text{f}}) - \Theta(\theta^-_{\max})]K^\infty = \eta F(\phi)K^\infty. \tag{26}$$

Eq. (26) quantifies the toughness increment from the frontal zone with

$$F(\phi) = \begin{cases} \frac{5}{2}\left(\sin\frac{\pi}{5}\cos\frac{12}{5}\phi + 2\sin\frac{2\pi}{5}\cos\frac{4}{5}\phi\right) & \phi \in \left[0, \frac{3}{8}\pi\right], \\ \frac{5}{2}\left(2\sin\frac{\pi}{5}\cos\frac{2\pi-4\phi}{5} + \sin\frac{2\pi}{5}\cos\frac{\pi-12\phi}{5}\right) & \phi \in \left(\frac{3}{8}\pi, \frac{\pi}{2}\right]. \end{cases} \tag{27}$$

The solution for $\phi \in [-\pi/2, 0]$ can be obtained by reflective symmetry (Yang and Zhu, 1998).

The contribution from the wake zone is explored under the case of the steady-state crack growth. The possibility of reverse switching is precluded in the wake for the sake of simplicity. In the wake, the contour zone of constant volume fraction takes on the shape of an infinite horizontal strip with a determined height. The equation of the strip and the corresponding area element are

$$r = h^\pm / \sin\theta^\pm, \quad \mathrm{d}A = h^\pm / \sin^2\theta^\pm \mathrm{d}\theta \mathrm{d}h. \tag{28}$$

Again, the first calculation explores the contribution from the wake of uniform switching. Toughness increment from the uniform upper wake is

$$\begin{aligned} \Delta K^{\text{uniform}}_{\text{wake}^+} &= \frac{3E\varepsilon_{\text{sp}}}{4\sqrt{2\pi}(1-\nu^2)} \int_0^{h^{\max}_{\text{transition}}} \int_{\theta^+_{\max}}^{\pi - \arctan\frac{h^+}{\Delta a}} V^0_{90} \sin\theta^+ \sin\left(\frac{5}{2}\theta^+ - 2\phi\right) \frac{\mathrm{d}\theta^+}{\sqrt{\sin\theta^+}} \frac{\mathrm{d}h^+}{\sqrt{h^+}} \\ &= \frac{EV^0_{90}\varepsilon_{\text{sp}}}{2\sqrt{2\pi}(1-\nu^2)} \int_0^{h^{\max}_{\text{transition}}} \left[f\left(\pi - \arctan\frac{h^+}{\Delta a}\right) - f(\theta^+_{\max})\right] \frac{\mathrm{d}h^+}{\sqrt{h^+}}, \end{aligned} \tag{29}$$

where

$$f(\theta^\pm) = \pm\sin\left(\frac{3}{2}\theta^\pm - 2\phi\right)(\pm\sin\theta^\pm)^{\frac{3}{2}}. \tag{30}$$

For the limiting case of a steady-state growing crack, one has

$$\lim_{h^+/\Delta a \to 0+} \int_0^{h^{\max}_{\text{transition}}} f\left(\pi - \arctan\frac{h^+}{\Delta a}\right) \frac{\mathrm{d}h^+}{\sqrt{h^+}} = \lim_{h^+/\Delta a \to 0+} \int_0^{h^{\max}_{\text{transition}}} -\cos 2\phi \left(\frac{h^+}{\Delta a}\right)^{\frac{3}{2}} \frac{\mathrm{d}h^+}{\sqrt{h^+}} = 0. \tag{31}$$

Combination of Eqs. (29) and (31) yields

$$\lim_{h^+/\Delta a \to 0+} \Delta K^{\text{uniform}}_{\text{wake}^+} = -\frac{EV^0_{90}\varepsilon_{\text{sp}}K^\infty}{32\pi(1-\nu^2)\sigma_{\text{th}}} \Psi(\theta^+_{\max}), \tag{32}$$

where

$$\Psi(\theta^{\pm}) = 8\sin\left(\frac{3}{2}\theta^{\pm} - 2\phi\right)\sin^4\theta^{\pm}. \tag{33}$$

The same procedure is carried out for the calculation of the uniform lower wake and the total contribution from the uniform wake is

$$\lim_{h/\Delta a\to 0}\Delta K_{\text{wake}}^{\text{uniform}} = \frac{EV_{90}^0\varepsilon_{\text{sp}}K^{\infty}}{32\pi(1-\nu^2)\sigma_{\text{th}}}[\Psi(\theta_{\max}^-) - \Psi(\theta_{\max}^+)]. \tag{34}$$

Similarly, the toughness increment from the non-uniform wake is

$$\lim_{h/\Delta a\to 0}\Delta K_{\text{wake}}^{\text{non-uniform}} = \frac{15(1-V_{90}^0)K^{\infty}}{32\pi(7-5\nu)}\ln\frac{\sigma_{\max}}{\sigma_{\text{th}}}[\Psi(\theta_{\max}^-) - \Psi(\theta_{\max}^+)]. \tag{35}$$

Combination of Eqs. (34) and (35) leads to

$$\lim_{h/\Delta a\to 0}\Delta K_{\text{wake}} = \eta[\Psi(\theta_{\max}^-) - \Psi(\theta_{\max}^+)]K^{\infty}. \tag{36}$$

Substitutions of Eqs. (26) and (36) into Eq. (25) yields

$$\Delta K = -\eta F(\phi)K^{\infty}. \tag{37}$$

for the steady-state toughness increment. As stated above, the reduction of Eq. (37) to the special case of uniform switching holds. Substituting Eq. (37) into (10) and applying the stress intensity factor criterion, one obtains the following non-dimensional relation

$$\frac{K^{\infty}}{K_{\text{intrinsic}}} = \frac{1}{1-\eta F(\phi)} \tag{38}$$

between the apparent fracture toughness and poling orientations. The relation is plotted in Fig. 4, where the upper curve refers to the result for cylindrical inclusion, and the lower curve refers to the result for spherical inclusion. Anisotropy of the apparent fracture toughness of ferroelectric induced by poling is verified quantitatively by Fig. 4.

4.3. Multiple domain orientations

After the acquisition of the mono-domain toughening solution, we shift our attention to ferroelectrics consisting of domains in different orientations. Barium titanate is chosen as a representative ferroelectric material in the subsequent discussion whose parameters will be described as follows. Orientation distribution function (ODF), $f(\phi)$, is introduced to describe domain orientations for ferroelectrics and it satisfies the normalized relation $\int_0^{\pi/2} f(\phi)\,\mathrm{d}\phi = 1$ in a plane texture. For un-poled ceramics, a completely random distribution exists and thus $f(\phi) = 2/\pi$. Hall et al. (2005) derived a poling-induced texture function in (100) plane, i.e. the fraction of domain having an orientation angle ϕ with respect to the whole domain of three different directions. Angle ϕ is measured between the domain orientation and the direction of the poling electric field, [100] direction, in the (100) plane. Hall et al. (2005) performed an in-plane XRD experiment to verify their theoretical analysis and the comparison indicated that the analysis agrees well with the measurement. They also developed a micromechanics model for the general three-dimensional case. For pre-poled barium titanate ceramics, Kolleck et al. (2000) measured a saturated poling strain of 0.15% experimentally. Combining this saturation poling strain, spontaneous strain in Appendix A and the in-plane version of the poling-induced texture model proposed by Hall et al., one may write

$$W(\phi) = \frac{1}{3} + 0.15\left(\frac{3}{2}\cos^2\phi - \frac{1}{2}\right). \tag{39}$$

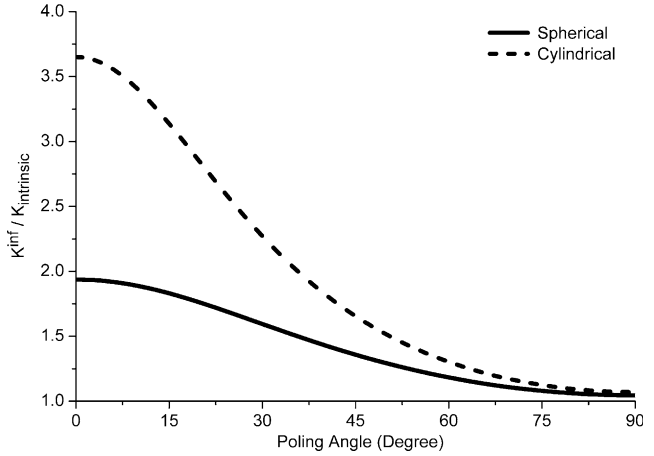

Fig. 4. Normalized remote stress intensity factors versus poling angle for spherical inclusion and cylindrical inclusion.

The orientation distribution function $f(\phi)$ appears to be

$$f(\phi) = W(\phi) / \int_0^{\frac{\pi}{2}} W(\phi)\,\mathrm{d}\phi. \tag{40}$$

The mono-domain solution and orientation distribution function can work together to give the apparent toughness as

$$K^{\infty} = \int_0^{\frac{\pi}{2}} K^{\infty}(\phi) f(\phi)\,\mathrm{d}\phi. \tag{41}$$

Reuss type approximation model is used in the estimation of (41) in ferroelectrics as described by Yang and Zhu (1998).

Some material parameters of barium titanate are listed below: $v = 0.35$, $E = 90$ GPa, $V_{90}^{\max} = 0.22$, and intrinsic fracture toughness $K_{\text{intrinsic}} = 0.74\ \text{MPa}\sqrt{\text{m}}$ (Kolleck et al., 2000). By solving (A.1) numerically, one obtains a threshold stress, σ_{th}, and uniform volume fraction, V_{90}^{0}, for spherical and cylindrical inclusions, as shown in Table 1. This Table also lists theoretical predictions for the asymptotes of R-curve under three cases: (1) ferroelectric samples poled parallel to the crack; (2) un-poled ferroelectrics; and (3) those poled perpendicular to the crack. The orientation distribution function for the first and the third case assumes the function form described by Eq. (40). Experimental plateau of R-curve for un-poled compact tension specimens of barium titanate is $1.12 \pm 0.06\ \text{MPa}\sqrt{\text{m}}$ (Kolleck et al., 2000). The experimental value lies between the predictions for spherical and cylindrical inclusions in Table 1. The prediction by spherical inclusion coincides better than that by cylindrical inclusion and thus the former seems to be favored.

Table 1
Switch-controlling parameters and predictions of apparent fracture toughness of different poling states by the spherical and cylindrical inclusions

	Spherical	Cylindrical
V_{90}^{0} (%)	1.8	3
σ_{th} (MPa)	10	9.25
K^{∞} (MPa$\sqrt{\text{m}}$)		
// Poled	1.10	1.59
Un-poled	1.05	1.46
$\perp$ Poled	1.00	1.33

Table 2
Theoretical predictions and experimental measurements of the maximum half-height of the intensive switching zone by spherical and cylindrical inclusions for ferroelectrics with three different poling states

	Spherical		Cylindrical
// Poled			
Prediction	23		34
Un-poled			
Prediction	16		29
Experiment		25	
⊥ Poled			
Prediction	11		23
Experiment		20	

The unit of all the quantities of this table is μm.

One may attribute the underestimate of spherical inclusions to the ignorance of out-of-plane non-uniform domain switching. The toughness calculation in this aspect by Yang et al. (2001a) clearly indicated additional toughening. The mismatch of the modulus between the matrix and the transitional switching zone may also contribute to the toughening.

From Fig. 4 and Table 1, one observes that the apparent fracture toughness for cylindrical inclusion shows much more poling-induced anisotropy than that for spherical inclusion. Since spherical inclusion model exerts more constraint than the cylindrical case, it is concluded that constraint determines the degree of anisotropy. The more the constraint is, the less the anisotropy will be. We then predict that the poling-induced anisotropy of apparent fracture toughness attains the utmost degree in ferroelectric single crystals.

Attention is finally focused on the size of domain switching zone under different poling conditions. Nomarski interference effect was utilized to visualize the process zone in situ during ferro-elastic domain switching around a crack tip (Förderreuther et al., 2002). Contour lines were recorded for the percentages of the switching events. The region where the switching percentage exceeded 50% was regarded as the zone where intensive switching occurred. They reported that the heights of such switching zones were 25 and 20 μm respectively for the un-poled and the perpendicularly poled samples (Förderreuther et al., 2002). From (B.3), it is seen that the maximum half-height depends on volume fraction and orientation angle. Before proceeding to further discussion, one needs to define two quantities possessed by the intensive zone. We assume the volume fraction within this zone exceeds half of the saturated value in the present non-uniform switching model. The maximum half-height of this zone is orientation dependent so one needs to define a critical angle to determine the expected size. The critical angle is settled such that the probability of the orientation interval ranging from zero to that angle equals 0.5 according to the ODF of Eq. (40). For the given volume fraction in the first assumption, the maximum half-height of any orientation in this interval is no less than that of the angle. Following these assumptions, our theoretical predictions for the maximum half-heights of the intensive switching zone for the paralleled poled, un-poled and perpendicularly poled cases are shown in Table 2. For the un-poled and perpendicularly poled cases, it is seen that experiment measurements fall into the interval defined by the predictions by the spherical inclusion and by the cylindrical inclusion. Again, the neglect of out-of-plane switching for the spherical inclusion model leads to an underestimate of the switching zone size.

5. Conclusions

This work introduces an evolution law of volume fraction for the switched domain and develops a new switching model for the non-uniform distribution of switching strain within the switching zone. Mono-

domain solution of toughening from non-uniform ferro-elastic domain switching is obtained for steady-state growing crack and is used to construct toughening for ferroelectrics with different poling states. Two sets of solutions for the toughening and the switching zone size are acquired for the spherical and the cylindrical inclusions. The interval defined by these solutions gives a good prediction of the corresponding experiment result for the toughening and the switching zone size.

Acknowledgements

This work was sponsored by the National Science Foundation of China under grant 10121202, as well as by the National 973 Project "Mechanics Modeling and Numerical Simulation of Meso-scale Properties of Materials" (grant 2004CB619304), and the "Sino-German Center for Research Promotion" under a project of "Crack Growth in Ferroelectrics Driven by Cyclic Electric Loading".

Appendix A. System energy of a switched ferroelectric grain

For a spherical grain with banded domain pattern constrained in an infinite matrix under remote electromechanical loading, the change in system energy due to banded domain switching is (Yang et al., 2001b)

$$\Delta U = \frac{E(7-5\nu)}{15(1-\nu^2)}\left(V_{90}\frac{c-a}{a}\right)^2 + \frac{4}{\pi}\sqrt{\frac{f(V_{90})\Gamma_{\mathrm{coh}}}{\pi D}\left[\frac{2(1-\nu)E}{(1+\nu)(3-4\nu)}\left(\frac{c-a}{a}\right)^2 + \frac{P_{\mathrm{s}}^2}{\varepsilon}\right]} - V_{90}\left[\frac{c-a}{a}(\bar{\sigma}_{22}-\bar{\sigma}_{33}) + P_{\mathrm{s}}(\bar{E}_2-\bar{E}_3)\right]. \tag{A.1}$$

Various parameters in (A.1) are explained below and are assigned definite values for the case of barium titanate. The barred quantities denote the remote loadings, such as $\overline{E}_i$ denote the applied electric field, and $\bar{\sigma}_{ij}$ the applied stress field ($i,j=1,2,3$). The spontaneous strain $(c-a)/a=0.01$, the spontaneous polarization intensity $P_{\mathrm{s}}=0.26\ \mathrm{C/m^2}$, the dielectric constant $\varepsilon=1900\varepsilon_0=1.68\times10^{-8}\ \mathrm{F/m}$ (Jaffe et al., 1971), the coherent domain wall energy $\Gamma_{\mathrm{coh}}=0.002\ \mathrm{J/m^2}$ (Lines and Glass, 1979), the grain size $D=15\ \mu\mathrm{m}$ (Kolleck et al., 2000), and the function $f(V_{90})=\sum_{k=1}^{\infty}\sin^2(V_{90}k\pi)/k^3$ (Yang et al., 2001b).

Appendix B. Angles and height in a switching zone

The conditions of $\sqrt{r}\geqslant 0$ determines the angular ranges of the switching zones in the upper half (labeled by a superscript "+") and the lower half (labeled by a superscript "−") as shown in (B.1), (B.2) and (B.4). The initial and the final angles marking those ranges are labeled by subscripts "i" and "f" respectively (Zhu, 1999; Yang, 2002).

$$\theta^+ \in \begin{cases} \left[\frac{4}{3}\phi, \frac{2}{3}(\pi+2\phi)\right] & \phi\in\left[0,\frac{\pi}{4}\right], \\ \left[\frac{4}{3}\phi,\pi\right] & \phi\in\left[\frac{\pi}{4},\frac{\pi}{2}\right], \end{cases} \tag{B.1}$$

$$\theta^- \in \begin{cases} \left[\frac{2}{3}(2\phi-\pi),0\right] & \phi\in\left[0,\frac{\pi}{4}\right], \\ \left[\frac{2}{3}(2\phi-\pi),0\right]\cup\left[-\pi,\frac{2}{3}(2\phi-2\pi)\right] & \phi\in\left[\frac{\pi}{4},\frac{\pi}{2}\right]. \end{cases} \tag{B.2}$$

The maximum half-heights h^+ and h^- in the upper half and the lower half planes can be determined by the conditions of $\mathrm{d}(r\sin\theta)/\mathrm{d}\theta=0$ as

$$h^{\pm} = \left(\frac{K_{\text{app}}}{2\sqrt{2\pi}\sigma_{\text{DS}}}\right)^2 |\sin\theta^{\pm}_{\max}|^5, \tag{B.3}$$

where the polar angles correspond to the maximum half-height of the switching boundary $\theta^{+}_{\max}$ and $\theta^{-}_{\max}$ are

$$\theta^{+}_{\max} = \frac{2}{5}(\pi + 2\phi) \;\; 0 \leqslant \phi \leqslant \frac{\pi}{2}, \quad \theta^{-}_{\max} = \begin{cases} \frac{2}{5}(2\phi - \pi) & 0 \leqslant \phi \leqslant \frac{3}{8}\pi, \\ \frac{2}{5}(2\phi - 3\pi) & \frac{3}{8}\pi \leqslant \phi \leqslant \frac{1}{2}\pi. \end{cases} \tag{B.4}$$

References

Budiansky, B., Hutchinson, J.W., Lambropoulos, J.C., 1983. Continuum theory of dilatant transformation toughening in ceramics. International Journal of Solids and Structures 19 (4), 337–355.

Bueckner, H.F., 1987. Weight functions and fundamental fields for the penny-shaped and the half-plane crack in three-space. International Journal of Solids and Structures 23 (1), 57–63.

Cao, H.C., Evans, G., 1993. Nonlinear deformation of ferroelectric ceramics. Journal of the American Ceramic Society 76 (4), 890–896.

Cox, B.N., Marshall, D.B., Kouris, D., Mura, T., 1988. Surface displacement analysis of the transformed zone in magnesia partially stabilized zirconia. Journal of the Engineering Materials and Technology—Transactions of the ASME 110, 105–109.

Förderreuther, A., Thurn, G., Zimmermann, A., Aldinger, F., 2002. *R*-curve effect, influence of electric field and process zone in $BaTiO_3$ ceramics. Journal of the European Ceramic Society 22, 2023–2031.

Gao, H., 1989. Application of 3-D weight functions-I. Formulations of crack interactions with transformation strains and dislocations. Journal of the Mechanics and Physics of Solids 37 (2), 133–153.

Hackemann, S., Pfeiffer, W., 2003. Domain switching in process zones of PZT: Characterization by microdiffraction and fracture mechanical methods. Journal of the European Ceramic Society 23 (1), 141–151.

Hall, D.A., Steuwer, A., Cherdhirunkorn, B., Withers, P.J., Mori, T., 2005. Micromechanics of residual stress and texture development due to poling in polycrystalline ferroelectric ceramics. Journal of the Mechanics and Physics of Solids 37 (2), 133–153.

Hannink, R.H.J., Kelly, P.M., Muddle, B.C., 2000. Transformation toughening in zirconia-containing ceramics. Journal of the American Ceramic Society 83 (3), 461–487.

Hsueh, C., Becher, P.F., 1988. Some consideration of nonideal transformation-zone profile. Journal of the American Ceramic Society 71 (6), 494–497.

Jaffe, B., Cook, W.R., Jaffe, H., 1971. Piezoelectric Ceramics. Academic Press, London and New York.

Kolleck, A., Schneider, G.A., Meschke, F.A., 2000. *R*-curve behavior of $BaTiO_3$- and PZT ceramics under the influence of an electric field applied parallel to the crack front. Acta Materialia 48, 4099–4113.

Lambropoulos, J.C., 1986. Shear, shape and orientation effects in transformation toughening. International Journal of Solids and Structures 22 (10), 1083–1106.

Lines, M.E., Glass, A.M., 1979. Principles and Applications of Ferroelectrics and Related Materials. Clarendon Press, Oxford.

Marshall, D.B., Shaw, M.C., Dauskardt, R.H., Ritchie, R.O., Readey, M.J., Heuer, A.H., 1990. Crack-tip transformation zones in toughened zirconia. Journal of the American Ceramic Society 73 (9), 2659–2666.

Reece, M.J., Guiu, F., 2002. Toughening produced by crack-tip-stress-induced domain reorientation in ferroelectric and/or ferroelastic materials. Philosophical Magazine A 82 (1), 29–38.

Rice, J.R., 1985. Three-dimensional elastic crack tip interactions with transformation strains and dislocations. International Journal of Solids and Structures 21 (7), 781–791.

Schäufele, A.B., Härdtl, K.H., 1996. Ferroelastic properties of lead zirconate titanate ceramics. Journal of the American Ceramic Society 79 (10), 2637–2640.

Yang, W., 2002. Mechatronic Reliability. Tsinghua University Press and Springer-Verlag, Berlin.

Yang, W., Zhu, T., 1998. Switch-toughening of ferroelectrics subjected to electric fields. Journal of the Mechanics and Physics of Solids 46 (2), 291–311.

Yang, W., Fang, F., Tao, M., 2001a. Critical role of domain switching on the fracture toughness of poled ferroelectrics. International Journal of Solids and Structures 38 (10–13), 2203–2211.

Yang, W., Wang, H.T., Fang, F., Cui, Y.Q., 2001b. Unconventional domain band structure at the crack tip in ferroelectric ceramics. Theoretical and Applied Fracture Mechanics 37, 397–408.

Yu, C.S., Shetty, D.K., Shaw, M.C., Marshall, D.B., 1992. Transformation zone shape effects on crack shielding in ceria-partially-stabilized zirconia (Ce–TZP)–alumina composites. Journal of the American Ceramic Society 75 (11), 2991–2994.

Zhu, T., 1999. Mechanics of electric field induced failure in ferroelectric ceramics. Ph.D. Thesis, Tsinghua University, Beijing (in Chinese).